Effect of Pressure on Skin-Electrode Impedance in Wearable Biomedical Measurement Devices

Bahareh Taji, Adrian D. C. Chan, *Senior Member, IEEE*, and Shervin Shirmohammadi, *Fellow, IEEE*

***Abstract*— Objective: This paper investigates the effect of applied pressure on the skin-electrode impedance. Applied pressure, which affects the skin-electrode impedance, can fluctuate in many acquisition setups, particularly in wearable devices. The skin-electrode impedance, in turn, impacts the quality of the recorded signal in biomedical monitoring devices. Methods: Three types of electrodes were examined: Ag/AgCl electrodes, conductive textile electrodes, and dry electrodes with surface microfeatures (Orbital Research Inc.). Impedance measurements were conducted as pressure was repeatedly applied (P = 4 kPa) and removed (P = 0 kPa) over several trials. A Cole–Cole impedance model was utilized to model the skin-electrode interface. Significance and Results: Results demonstrated large decreases in the skin-electrode impedance of dry electrodes (conductive textile and orbital electrodes), especially with the initial application of the pressure. Model parameters also proved to be highly dependent on the level of pressure in dry electrodes but less dependent and more stable in wet electrodes. Decreases in skin-electrode impedance associated with applied pressure were thought to be caused by an increased effective electrode contact area. Changes in skin-electrode impedance were irreversible, lasting even after the applied pressure was released. Differences skin-electrode impedance associated with changes in applied pressure, decreased as the number of trials increased. Conclusion: Applied pressure has larger effect on dry electrodes than wet electrodes. Wearable devices that employ dry electrodes may have poorer biomedical signal quality when initially donned; however, the advantage of wet electrodes with their lower sensitivity to applied pressure is diminished in long-term monitoring applications.**

***Index Terms*— Biopotential electrodes, biosignal, Cole-Cole impedance model, impedance, pressure, signal quality, skin electrode.**

I. Introduction

A NEW generation of devices potentially transforming the biomedical monitoring industry is patient-empowering, information-leveraging technologies [1]. Such devices provide relevant information and analyses directly to users, enabling real-time feedback. One major class of such products are wearable devices, which can enable continuous measurement of biosignals [e.g., electrocardiogram (ECG) and electromyogram (EMG)], and can provide useful information regarding the function and status of the body. Health IT leaders need to embrace this sort of innovations, including home healthcare devices, because they solve some critical and prevalent challenges, such as the increasing cost of healthcare, the aging population, and the shortage of healthcare professionals. In addition to healthcare applications, wearable devices are utilized in fitness, well-being, and performance monitoring to provide information for healthy people via devices such as smartphones [2]. Hence, wearable devices also support healthy users and their active lifestyles and more importantly empower people to detect early any health risk or disorders [2].

In [3], the main applications of wearable devices were categorized into five groups: health and wellness monitoring, safety monitoring, home rehabilitation, assessment of treatment efficacy, and early detection of disorders. Cloud-based services further increase the value of such wearable monitoring devices (see [4], [5]).

A common functionality of these devices is to acquire biosignals. Biosignals can be acquired noninvasively using biopotential electrodes placed on the surface of the skin. These biopotential electrodes then serve as the transducers between the body and the measurement device. Selection of an appropriate electrode is important for ensuring a good quality signal; however, potentially competing considerations are usability factors. Disposable nonpolarizable biopotential electrodes (e.g., Ag/AgCl) may be preferable in a clinical environment for individual, short-term monitoring tests; whereas, reusable, washable dry electrodes are preferred in wearable devices. While dry, polarizable electrodes have traditionally been thought to have poor performance compared to wet, nonpolarizable electrodes, research has demonstrated that the recorded signal quality can be comparable [6], [7].

The skin-electrode impedance plays a major role in the quality of biosignal recording [8], [9]. Many wearable devices use some sort of elastic material to conform to the body shape and to provide pressure in order to ensure good contact between the skin and the electrode. Electrodes can be integrated in this manner into a variety of wearable form factors, including belts, bands, shirts, and pants. Tighter fitting clothing may increase the applied pressure, decreasing the skin-electrode impedance, which in turn improves the quality of biosignal recordings, but they may also reduce comfort, especially during extended recording periods. In addition, muscle contractions and respiration can alter the body volume under the electrodes; this would affect the tightness of clothing,

Manuscript received November 1, 2017; revised January 30, 2018; accepted February 1, 2018. Date of publication March 20, 2018; date of current version July 12, 2018. The Associate Editor coordinating the review process was Dr. Domenico Grimaldi. *(Corresponding author: Bahareh Taji.)*

B. Taji and S. Shirmohammadi are with the School of Electrical Engineering and Computer Science, University of Ottawa, ON K1N 6N5, Canada (e-mail: btaji016@uottawa.ca; shervin@eecs.uottawa.ca).

A. D. C. Chan is with the Department of Systems and Computer Engineering, Carleton University, Ottawa, ON, Canada (e-mail: adcchan@sce.carleton.ca).

Color versions of one or more of the figures in this paper are available online at http://ieeexplore.ieee.org.

Digital Object Identifier 10.1109/TIM.2018.2806950

modulating the applied pressure on the electrode, which in turn would modulate the skin-electrode impedance. Changes in the skin-electrode impedance can affect the quality of biosignal recordings and can result in measurement contaminants, such as motion artifact [9], [10]. In [11], it was shown that QRS detection is influenced by the skin-electrode impedance and its effects causes a risk of misinterpretation of the ECG. Similar issues were noted for ECG acquisition in ambulatory assistive devices, where electrodes were integrated in the handles of a rollator, and the grip and loading forces varied during recordings [12]. Skin-electrode impedance information could be applied as an indication of motion artifact [13] and can be used in adaptive methods to mitigate motion artifact [14].

In this paper, we extend our previous study in [15], where we measured the skin-electrode variation, as pressure was applied, for one electrode type (conductive textile) and for three subjects. In that research, impedance was measured as pressure was stepwise increased to a high pressure (16 kPa); the context of this previous work was blood pressure monitoring with ECG. In this paper, we examine applied pressure and its impacts on the skin-electrode impedance in the context of wearable devices. Three electrode types are examined as pressure is repeatedly applied and removed over several trials and for six subjects. We also verify the reversibility of the skin-electrode impedance variations before applying pressure and after removing it. An electric circuit is used to model the electrode impedances to better understand the resultant changes in the skin-electrode impedance. The main contributions of this paper can be summarized as follows.

1) Studying the variation of the skin-electrode impedance associated with three electrode types: Ag/AgCl electrodes, conductive textile, and orbital electrodes under pressure. We propose a data acquisition procedure and pressure applying method in order to measure the skin-electrode impedance variation with and without applying pressure. All measurements are performed for six subjects. We will demonstrate how the impedance changes when pressure is applied and removed. Results obtained from all electrode types are compared.
2) We parameterize the skin-electrode impedance with the Cole–Cole impedance model [16], [17]. We extract these components of the skin-electrode impedance and measure their variation rate in response to applying pressure. We investigate how each component varies in each electrode type and compare them.
3) Irreversible changes in the skin-electrode impedance and its corresponding components that occur due to applying pressure is also verified in three electrode types and they are compared in terms of the extent they sustain the changes after we remove the pressure. Within this paper, the term "irreversible changes" refers to observed changes in the skin-electrode impedance, due to applied pressure, that do not return to their original values when the applied pressure is removed (at least within the observed time period, which was several minutes).

The rest of this paper is organized as follows. In Section II, we present some literature review in this field and also skin-electrode impedance models. In Section III, we explain our methodology, including the electrodes we utilize, devices we employ for data acquisition, the process we arranged to acquire data as well as our pressure applying method. Section IV contains the results and discussion, comparing different types of electrodes in terms of their behavior under pressure. Conclusions are presented in Section V.

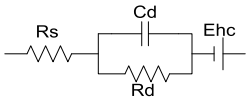

Fig. 1. Single-time-constant skin-electrode interface model.

II. Related Work

A. Skin-Electrode Impedance Modeling

Skin-electrode impedance is the impedance between the body and the electrode which plays a major role in the quality of the signal sensed by the electrode [9], [11], [18]. A low skin-electrode impedance is desired, because higher skin-electrode impedances are associated with a lower signal-to-noise ratio and increased susceptibility to artifacts and interference [19], [20].

An electrical circuit model can be helpful in order to better understand and analyze the skin-electrode impedance behavior. Warburg [21] was the first to propose such circuit model for the electrode–electrolyte interface; however, Helmholtz was the one who proposed that a double layer of charge occurred in this interface [22]. Assambo *et al.* [23] identified the components of the electrode circuit model, analyzing its electrical properties in ac and dc measurements. Their study helped in estimating the values of capacitors and resistors in the skin-electrode electrical model. Three popular electrical models suggested for skin-electrode interface are: 1) the single-time-constant model; 2) the double-time-constant model; and 3) the Cole–Cole model.

1) Single-Time-Constant Model: Recognizing limitations with the Warburg model which includes one resistor and one capacitor, Geddes [22] suggested a model for the skin-electrode impedance, which is a combination of a resistor in series with a paralleled resistor and capacitor as shown in Fig. 1, where E_{hc} is the half-cell potential, C_d is the capacitance between the electrode and the skin [19], [24], R_d is the resistance between the skin and electrode during charge transfer [19], [24], and R_s represents the total resistance of electrolyte gel (if any), sweat, and also the underlying skin tissue [20], [25]. This model is known as the single-time-constant model [19] and implies that the total impedance is frequency dependent. At low frequencies, the capacitor (C_d) acts like an open circuit, thus impedance approaches $R_s + R_d$. At high frequencies, C_d acts like a short circuit resulting in an impedance that approaches R_s.

2) Double-Time-Constant Model: Kaczmarek and Webster [26] suggest a more complicated model for the skin-electrode impedance. As depicted in Fig. 2, it is actually composed of two stages of the single-time-constant model and is known as the double-time-constant model. The first stage

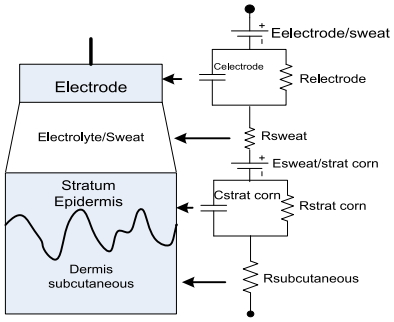

Fig. 2. Double-time-constant model, based on [23].

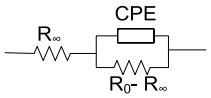

Fig. 3. Cole–Cole model schematic view [28].

represents the electrode–electrolyte interface. The second stage represents the electrolyte-skin interface. In [23], both models are explored in terms of ECG measurement and frequency response, and the findings show that the double-time-constant model exhibits more accurate results.

3) Cole–Cole Model: The Cole–Cole impedance model is a popular impedance model, especially for biological tissues [16], [17]. It is applied as skin-electrode contact impedance since the impedance of skin dominates the total impedance in a double-layer (double-time-constant) model [27]. It is similar to single-time-constant model. The difference is that instead of C_d there is a constant phase element (CPE), which is also known as the fractional capacitor [28]. The impedance of this component is equal to

$$Z_{\text{CPE}} = 1/(j\omega C)^{\alpha}$$

where C is the capacitance and α is its order ($0 < \alpha <= 1$) [28]. Fig. 3 presents the model equivalent circuit diagram. In this paper, we use the Cole–Cole model instead of other options such as the single-time-constant model, because the frequency response represented by the Cole–Cole model's CPE element is more elaborate than other models [29] and is able to better model the observed impedances. In this paper, we use the four components of this model (C, R_0, R_∞, and α) to explore each electrode's behavior under pressure.

B. Skin-Electrode Impedance Measurement

Skin-electrode impedance has always been of interest because it is an important factor in biosignal quality. Thus, many papers in the literature have discussed measurement methods for the skin-electrode impedance and methods to improve the measurement accuracy. A method with the measurement setup shown in Fig. 4 is proposed in [30]. In this method, three electrodes are applied on the arm, and the skin-electrode impedance of the electrode in the middle is calculated. The current flowing between A and B can be calculated by measuring the voltage drop in E_r. A buffer unit is utilized to prevent any significant current flow between

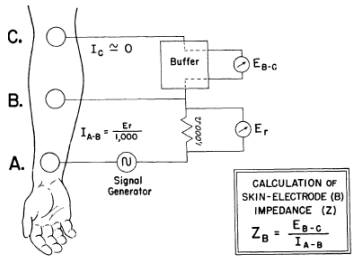

Fig. 4. Skin-electrode impedance measurement setup [30].

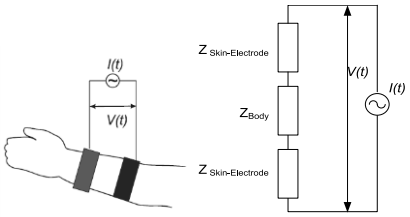

Fig. 5. Two electrode configuration for skin-electrode impedance measurement [31].

electrodes B and C (i.e., $I_c \approx 0$). Furthermore, a known sine wave is applied to electrode B and the voltage between B and C is measured. Thus, impedance of B can be obtained using the following equation:

$$Z_B = \frac{E_{B-C}}{I_{A-B}}.$$

Another method is presented in [31], which employs a two-electrode configuration, as shown in Fig. 5. Two electrodes are applied on the forearm and a known sine current is injected and the voltage drop between the electrodes is measured. In this setup, the skin-electrode impedance of both electrodes plus body impedance is measured; assuming the skin-electrode impedances are equal and the body impedance is negligible, the resultant measurement can be simply divided by two to obtain the impedance for one electrode.

C. Effects of Applying Pressure

Skin-electrode impedance is affected by a variety of factors including electrode material [6], [32], electrode size [6], [33], skin preparation [34]–[36], skin type [37], [38], sweat secretion [37], [39], heat [40], [41], and atmospheric humidity [41]. An external pressure or force, applied to the electrode, has also been shown to influence the skin-electrode impedance [42], [43].

It has been generally observed that increasing the applied pressure is associated with a decrease in the skin-electrode impedance [15], [42], [44]. The effect of externally applied pressure not only depends on the electrode type [45], [46], but also varies from person to person [44], [45]. A hysteresis effect was observed in [42] and [44], where applying pressure to the electrodes caused irreversible decreases in the skin-electrode impedance. In [44], skin-electrode measurements were performed on only two subjects, using large applied forces that are not representative for wearable devices.

Similar results were also found in [43] where it is noted that the skin-electrode impedance is influenced by the applied force, and that the larger force or pressure we apply, the more skin-electrode impedance decreases. The objective of this paper was to introduce a new type of dry and capacitive electrode appropriate for long-term ECG monitoring. Although, this paper reported some observations regarding the impact of applied pressure on their electrodes, these effects on the skin-electrode impedance were not of main concern. Unfortunately, limited details are provided with regards to the methodology of applying pressure, the skin-electrode impedance measurement method, and its variation under pressure, making it difficult to evaluate these findings.

In [42], the application area of interest was impedance plethysmography rather than biosignals; the results only included the skin-electrode impedance values at 5 kHz, well-above the bandwidth for noninvasive biosignals. While [47] was also directed toward impedance plethysmography, skin-electrode impedances for Ag/AgCl, aluminum (Al), and silver (Ag) electrodes were measured between 1 Hz and 1 MHz. Measurements were performed for one subject, so the repeatability and generalizability of the findings is unknown. In [42] and [47], a decrease in the skin-electrode impedance was associated with increased applying pressure. In addition, larger decreases in the skin-electrode impedance were noted for dry electrodes than for wet electrodes, where an electrolytic gel is employed. Smaller changes in the skin-electrode impedance were noted in [47] compared to [42]; these differences were attributed to differences in how the electrodes were initially applied [47]. Such inconsistencies point to the need for further research.

III. Methodology

A. Electrodes

Three types of electrodes are utilized in this paper:

1) Ag/AgCl surface electrodes (Model T-00-S/25, Ambu Blue Sensors T);
2) conductive textile electrodes; (Medical grade silver % nylon and 8% dorlastan stretchable conductive fabric with the thickness of 0.50 mm, which offers the unique ability to stretch in both directions. This fabric stretches to 100% in length and 65% in width. Its surface resistivity is less than 1 Ω/m^2 when unstretched.)
3) orbital electrodes (Orbital Research Inc., Cleveland, OH, USA).

All three are shown in Fig. 6 and are referred to in this paper as Ag/AgCl, conductive textile, and orbital electrodes, respectively. The Ag/AgCl electrodes are wet electrodes, pregelled with an electrolytic gel, whereas conductive textile and orbital electrodes are dry electrodes. These Ag/AgCl electrodes have a diameter of 10 mm and are used extensively in research and in clinical practice, including EMG and ECG recordings. Conductive textile electrodes are basically made of silver coated nylon filaments (AgNy). Each textile electrode is a 3 cm $\times$ 30 cm strip and is wrapped around the subjects' biceps during the measurement procedure. These electrodes have been used in wearable devices and also for collecting ECG, EEG, and EMG signals for research purposes. The orbital electrodes have a diameter of 25 mm, and have an array of microfeatures that embed themselves in the stratum corneum layer of the skin. The objective of these microfeatures is to circumvent the need for an electrolytic gel or skin preparation [48]. These electrodes are targeted for ECG acquisition. A larger sized electrode results in a larger contact area, which leads to smaller absolute impedance. We mainly investigate relative impedance changes to account for size differences between electrode types.

Fig. 6. Electrodes used in this paper (a) Ag/AgCl, (b) conductive textile, and (c) orbital electrodes.

B. Measurement Setup

Skin-electrode impedance was measured with a pair of electrodes that were placed above the right biceps. Electrodes were spaced 7 cm apart. For the Ag/AgCl and orbital electrodes, a snap electrode lead was used to interface the electrodes to the impedance measurement system. For the conductive textile electrode, we used an alligator clip connector between the electrode and the measurement system, which tightly held the fabric to establish a robust electrical connection. Since our objective is to simulate the use case of a home health care device, we avoided the use of skin preparation. While skin preparation would improve the skin-electrode impedance, it can be a barrier to use by nonexpert users due to issues such as comfort, convenience, and time. The Omron Heart scan and the FavoritePlus Easy ECG are examples of popular portable ECG recording devices that do not instruct users to perform any skin preparation. Various electrode types, including conductive textiles, have shown good promise in delivering adequate signal quality without skin preparation [7], [49], [50]. From a usability standpoint, wearable devices that do not require skin preparation are ideal and more easily accepted by users. The literature also suggests that adequate signal quality can be obtained without any skin preparation [6], [7], [49], [51]. Orbital electrodes, used in this paper, were in fact designed to avoid the need for skin preparation [52]. It is also noted that no significant amount of hair was observed at the electrode sites (anterior part of arm, above the biceps) for any of the subjects who participated in this paper. We also measured the skin-electrode impedance of one subject, with and without skin preparation; results are presented in Fig. 7. As expected, the measured impedance for each electrode with skin preparation is lower than the impedance without skin preparation; however, differences were not large.

We utilized commercially available state-of-the-art devices that are designed specifically for this purpose in order to measure the skin-electrode impedance variation over a particular

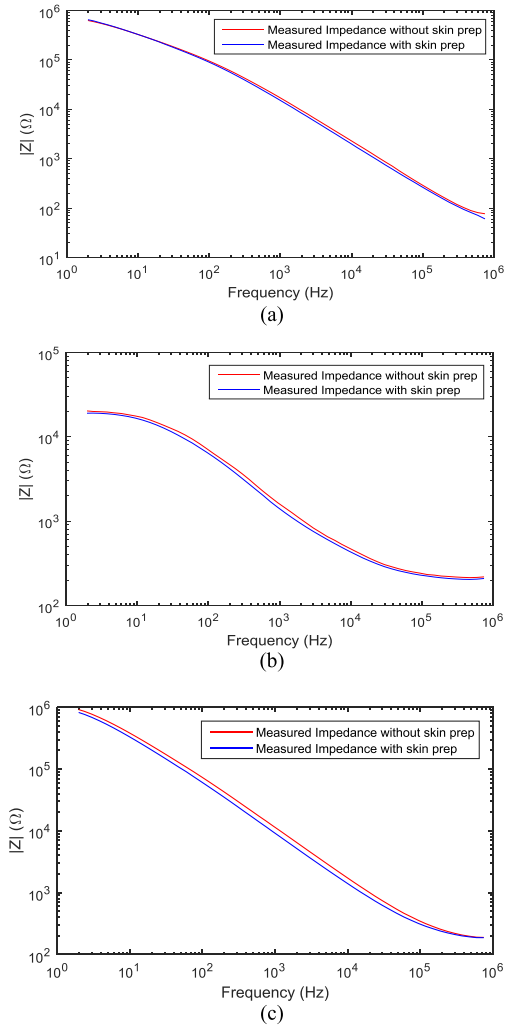

Fig. 7. Measured impedance with and without skin preparation (a) Ag/AgCl, (b) conductive textile, and (c) orbital electrodes.

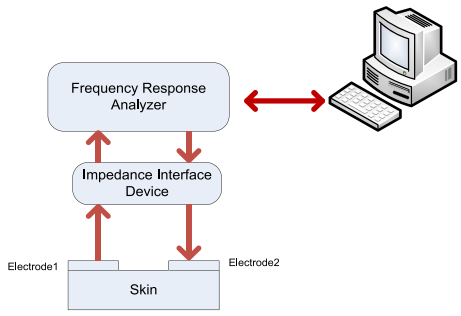

Fig. 8. Experimental setup for skin-electrode interface measurement.

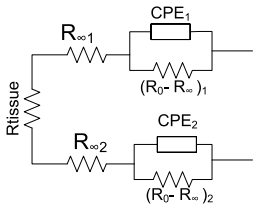

Fig. 9. Schematic view of skin-electrode impedance measurement.

TABLE I
SUBJECTS' CHARACTERISTICS

	Sex	Height(cm)	Weight(Kg)	BMI	Age
Subject1	Female	172	68.0	23.25	36
Subject2	Female	163	70.3	26.45	26
Subject3	Male	177	95.0	30.32	66
Subject4	Female	163	47.0	17.69	28
Subject5	Male	177	71.0	22.66	35
Subject6	Female	164	72.8	27.06	31

frequency range. A block diagram of the experimental setup is shown in Fig. 8. This represents a two-electrode configuration that includes a frequency response analyzer (Model 1255B, Solartron Analytical, U.K.) and an impedance interface device (Model 1294A, Solartron Analytical, U.K.), as well as a personal computer. Skin-electrode impedance was measured, using a 100-μA ac current. We measure 10 points per decade, averaging 30 cycles per frequency, sweeping the frequency from 750 KHz down to 2 Hz. Each impedance measurement took approximately 2 min to complete. The impedance measurement includes impedance of the two electrodes plus the underlying tissue impedance, which is modeled in Fig. 9.

Measurements were carried out on six healthy subjects (four females, two males). None of the volunteers were taking any medication or had a known history of cardiovascular disease. Table I shows subjects' characteristics in terms of sex, height, weight, body mass index, and age. The research was reviewed and approved by the Carleton University Research Ethics Board.

1) Applying Pressure to the Electrodes: In order to investigate the effects of applying pressure to the electrodes, we designed our own system for applying pressure using a blood pressure cuff. This system consists of a microprocessor (CC2531F256, Texas Instruments), a motor, a bleed valve, a pressure sensor (26PC series, Honeywell), and an Omron blood pressure cuff. We apply pressure by inflating the cuff while the electrodes are located underneath the cuff. The pressure sensor is sensing the pressure inside the cuff, which the microprocessor uses to turn ON the motor to inflate the cuff to the desired pressure and maintain the pressure due to any pressure leakage in the system. Therefore, we have a constant level of pressure during each measurement.

2) Experimental Procedures: Each electrode type is tested separately for six subjects. Measurements are done first for Ag/AgCl electrodes. Then one day after that, we repeated the procedure for conductive textile and orbital electrodes. There was a 5 min waiting period between conductive textile and orbital electrodes measurements. A new Ag/AgCl electrode was used each time; whereas the other electrodes were reused. The electrodes and the blood pressure cuff were placed on the subject's bicep. The impedance was measured in 11 trials with the cuff pressure in each trial shown in Table II. The first eight trials the cuff was alternating between 0 Pa and 4 kPa. In the last three trials, the pressure was kept at 0 Pa to observe the reversibility of pressure loading effects on the skin-electrode impedance. There was a 1 min waiting period between each

TABLE II
CUFF PRESSURE PER TRIALS

Trial	T1	T2	T3	T4	T5	T6	T7	T8	T9	T10	T11
Cuff pressure (Pa)	0	4k	0	4k	0	4k	0	4k	0	0	0

two consecutive measurement trials. The entire measurement procedure is summarized as follows.

1) Both electrodes are placed on the subject's right bicep at a 7-cm distance from each other and connected to the Solartron devices.
2) The Omron cuff is wrapped around subject's bicep on top of the electrodes.
3) The pressure is set to 0 Pa or 4 kPa appropriate for the trial (Table II).
4) Wait for 1 min.
5) The impedance is measured by the Solartron device (∼2 min).
6) Repeat, starting from step 3, until all trials are completed.

C. Skin-Electrode Impedance Modeling

The parameters of the Cole–Cole model are estimated for each impedance measurement. As noted in Section II-B, the impedance measurements include the skin-electrode impedance of two electrodes and the impedance associated with the body tissue between the electrodes. Since the electrodes we apply are identical in terms of type, material, and size, we assume that they have equal skin-electrode interface impedance [i.e., $C = C_1 = C_2$, $\alpha = \alpha_1 = \alpha_2$, $R_\infty = R_{\infty 1} = R_{\infty 2}$, $R_0 - R_\infty = (R_0 - R_\infty)_1 = (R_0 - R_\infty)_2$]. The resistance of tissues between two electrodes R_{tissue} is expected to be small; a value of approximately 150 Ω was measured at the middle of the upper arm [32]. Here, we assume $R_{\text{tissue}} = 0$, so any tissue impedance will be integrated into the estimate of R_∞. Therefore, the skin-electrode impedance for a single electrode is considered as the measured impedance value divided by two.

A least-squares nonlinear curve fitting method is used to estimate the model parameters (C, α, R_∞ and R_0) from the skin-electrode impedance measurements. The curve fitting algorithm required the initialization of each parameter. According to the electrical model, at high frequencies the impedance approaches R_∞, and as the frequency approaches zero, the impedance approaches R_0. Applying this fact, the initial value for R_∞ is set as the impedance measured at the highest frequency [$R_{\infty\text{INIT}} = Z(750\text{ kHz})$]. The initial value for $R_0 - R_\infty$ is set as the impedance measured at the lowest frequency, less R_∞, [$R_{0\text{INIT}} = Z(2\text{ Hz})$]. It should be mentioned that τ is known as the characteristic time constant of the impedance and is equal to $[(R_0 - R_\infty)C]^{1/\alpha}$ [28]. In order to calculate α, first we need to find φ_{CPE} as shown in Fig. 10 which is an impedance plot of the imaginary component (Z'') versus the real component (Z'). R_∞ and R_0 can be directly found from the curve and the angle $\varphi_{\text{CPE}} = \alpha\pi/2$ allows us to calculate α

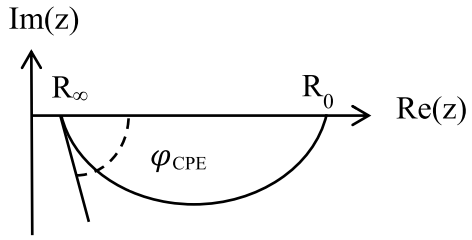

Fig. 10. Impedance loci used to extract parameter set (R_0, R_∞, τ, α) (based on [28]).

$$Z(\omega) = R_\infty + \frac{R_0 - R_\infty}{1+(j\omega\tau)^\alpha} = Z' + jZ''$$

and

$$(j\omega)^\alpha = \omega^\alpha\left[\cos\left(\frac{\alpha\pi}{2}\right) + j\sin\left(\frac{\alpha\pi}{2}\right)\right]$$

Therefore, α is known and we take it as its initial value (α_{INIT}) and on the other hand, real part of the impedance (Z) has its maximum value at the frequency of $1/\tau$. Therefore, we can compute τ which is also equal to $[(R_0 - R_\infty)C]^{1/\alpha}$. C is found to be $\tau/(R_0 - R_\infty)$ and the calculated value of C is also taken as its initial value (C_{INIT}).

Employing this procedure enables us to find the values of $R_\infty, R_0 - R_\infty, \alpha$, and C for each measurement.

We picked an impedance measured in one of our trials for one of subjects (subject 1, trial 1, conductive textile electrode) randomly to illustrate the curve fitting. The least-squares curve fitting on the experimental data from that trial returned the following values for the three components:

$$R_\infty = 207.5\ \Omega,\ \ R_0 = 1.08\ \text{M}\Omega,\ \ C = 1.92\ \text{nF},\ \ \alpha = 0.942$$

In order to compare the obtained data and observed one, we substituted the values of the components in (1), which shows the mathematical relation between $|Z(\omega)|$ and its four components including R_0, R_∞, α, and C. Fig. 11(a) illustrates the result graph of obtained $|Z(\omega)|$ and observed graph data on the same plane for comparative purposes and Fig. 11(b) and (c) visualize our model and observed data real and imaginary parts, respectively

$$Z(\omega) = R_\infty + \frac{R_0 - R_\infty}{1+(j\omega)^\alpha(R_0 - R_\infty)C} = Z'(\omega) + jZ''(\omega) \tag{1}$$

IV. EXPERIMENTAL RESULTS

In this paper, we expand our preliminary measurements done for three subjects and one electrode type (conductive textile) [15]. We perform the measurements for more subjects and three different types of electrodes to compare their behavior when applying pressure and discuss their appropriateness for use in wearable devices. According to this and to achieve our objective in terms of comparing different parameters in obtained results, we present them as follows.

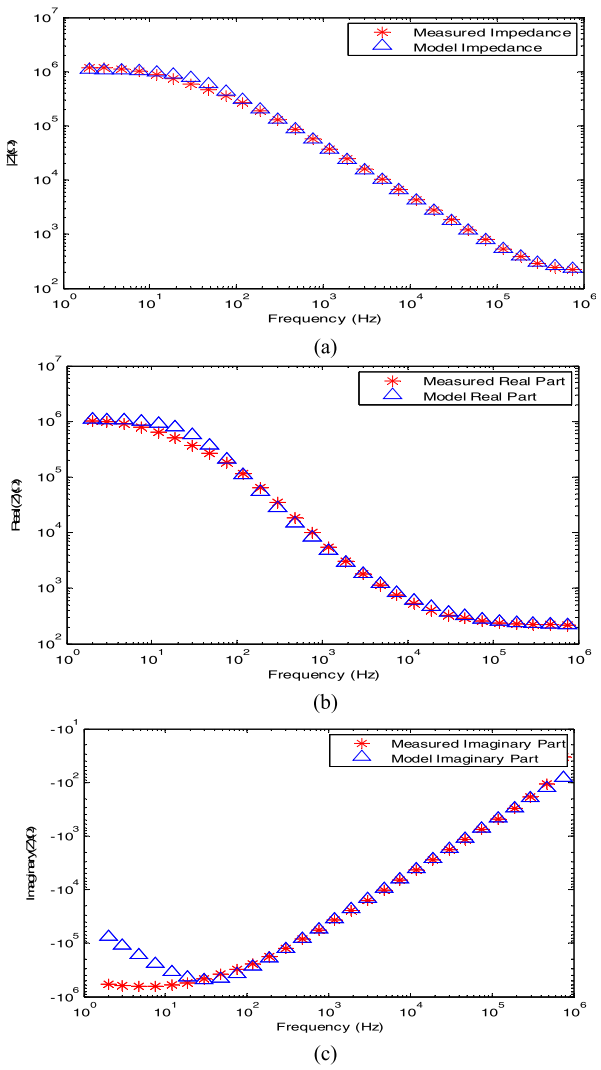

Fig. 11. (a) Measured impedance and the corresponding skin-electrode model impedance. (b) Real part of measured and model impedance. (c) Imaginary part of measured and model impedance.

1) Skin-electrode impedance across five trials (trials 1, 2, 7, 8, and 11), one subject (subject1), and three electrode types (Fig. 11).
2) Skin-electrode impedance variation in 30-Hz frequency, for 11 trials, three electrodes types, and six subjects (Fig. 12).
3) Reversibility of the skin-electrode impedance (Table III).
4) Component C variation in 11 trials, six subjects, and three electrode types. C is normalized to its value in the last trial (Fig. 13).
5) Component R_0 variation in 11 trials, six subjects, and three electrode types. R_0 is normalized to its value in the last trial (Fig. 14).
6) Component R_∞ variation in 11 trials, six subjects, and three electrode types. R_∞ is normalized to its value in the last trial (Fig. 15).
7) Component α variation in 11 trials, six subjects, and three electrode types. α is normalized to its value in the last trial (Fig. 16).
8) Reversibility of the skin-electrode impedance components (Tables IV and V).

The reason why we picked trial 11 and not trial 1 for normalizing values is that trial 11 better represents the "settled" skin-electrode impedance and it is more important to know how the impedance is relative to this value. Another reason is that impedance measured in trial 1 would be highly variable because it is the initial application of the electrode. If for example, the initial application was very poor with little skin-electrode contact, the initial impedance would be extremely high and normalizing to this would make all other values a really small percentage.

Fig. 12 depicts the magnitude of the skin-electrode impedance for Subject 1 for three electrodes, showing the skin-electrode impedance of the first and last 0 Pa/4 kPa pair (trials 1, 2, 7, and 8), and the last trial (trial 11). All electrodes have lower impedance when pressure is applied for the first time (trial 2) compared to their initial state (trial 1) and this is consistent with what we observe in the last 0 Pa/4 kPa pair (trials 7 and 8). However, we observe a smaller change in the last 0 Pa/4 kPa pair compared to the first 0 Pa/4 kPa pair. Skin-electrode impedance value in the last trial (trial 11) is close to its value in the last pressure applying trial (trial 8) which shows the irreversible changes in the skin-electrode impedance after several pressure loading and unloading trials. Ag/AgCl electrode shows the smallest value of the skin electrode impedance and also the smallest amount of variation due to applying pressure (Fig. 12). The conductive textile has the largest skin-electrode impedance and shows the largest amount of variation before and after applying pressure. The low variation in the skin-electrode impedance for Ag/AgCl electrodes and relatively high variation for conductive textile electrodes was consistent for all subjects.

Fig. 13 depicts the magnitude of the skin-electrode impedance measured at 30 Hz for six subjects, for all electrode types. We pick 30 Hz because our interest is studying effects of electrodes on biosignals, which are of low frequencies. In addition, many commercial electrode impedance meters test at this frequency.

For all electrodes and subjects, the impedance generally decreases with increasing trials. Ag/AgCl electrodes show the smallest variation among three electrode types and the impedance does not change dramatically with and without pressure [Fig. 13(a)].

For conductive textile, an obvious pattern with increased pressure is observed, where applying pressure decreases impedance and removing pressure increases it [Fig. 13(b)]. This pattern is present but less obvious with orbital electrodes [Fig. 13(c)]. Such a pattern is not visible with Ag/AgCl [Fig. 13(a)]. Larger changes in impedance are experienced in earlier trials and maximum decrease is associated with the initial pressure application (trial 2). The fluctuations of the impedance become smaller and smaller after each pressure trial compared to the last pressure trial.

This is to be expected as no skin preparation was done and so the skin-electrode contact is expected to be initially poor, which can be improved with applied pressure. As well,

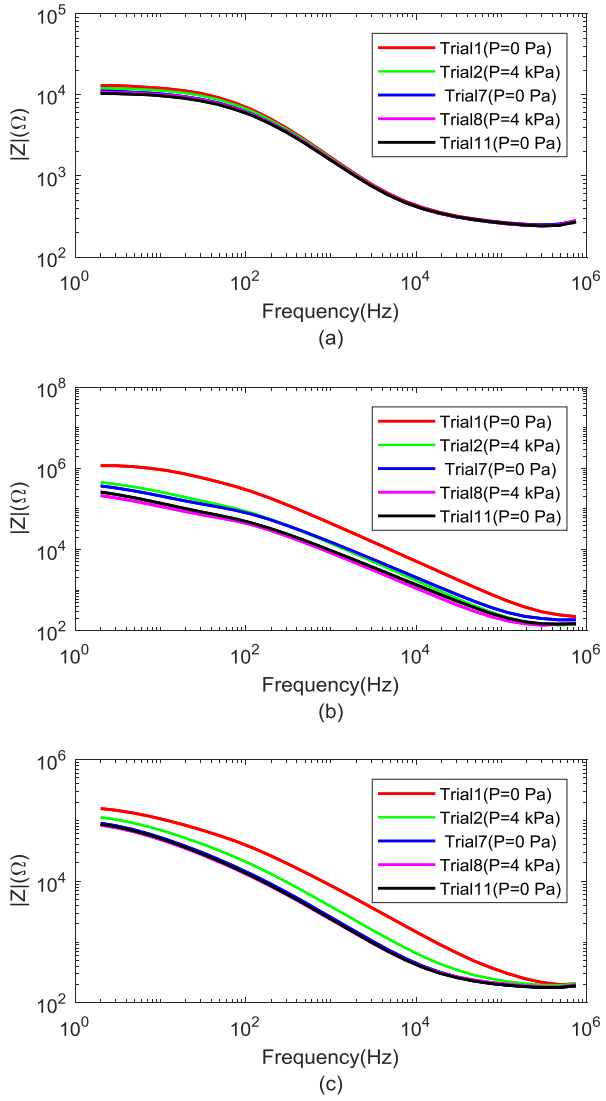

Fig. 12. Skin-electrode impedance for three electrodes, Subject1 (a) Ag/AgCl, (b) conductive textile, and (c) orbital electrodes.

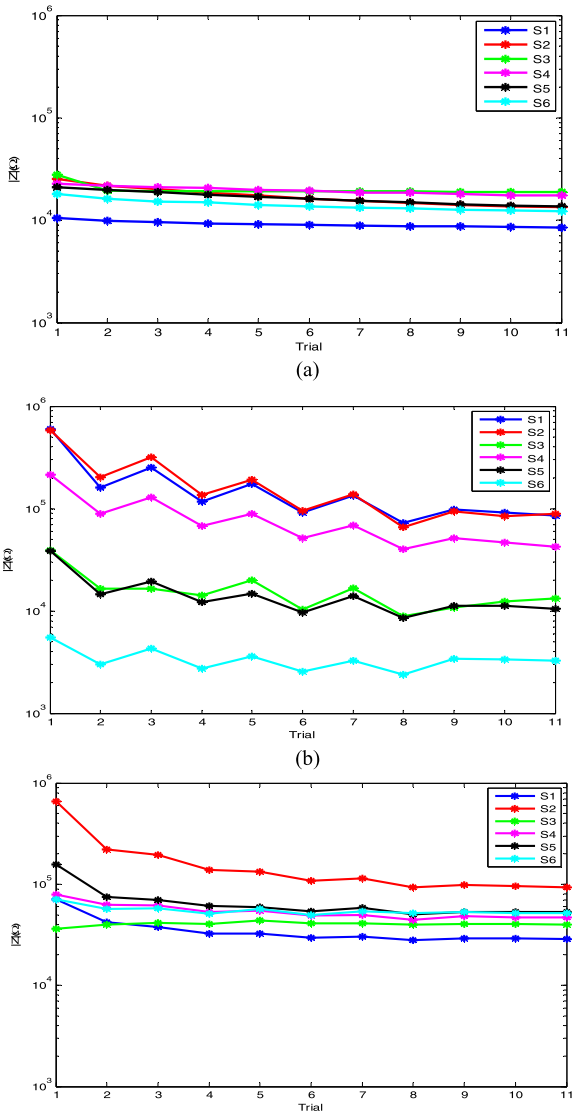

Fig. 13. Measured impedance at $f = 30$ Hz (a) Ag/AgCl, (b) conductive textile, and (c) orbital electrodes.

there is electrode settling, where the skin-electrode impedance decreases with time. In last three trials, which are all done without applying pressure, there is a little change compared to the last pressure trial (trial 8). This suggests that effects are irreversible from their initial state and any electrode settling is relatively stable by trial 8. Table III shows all electrodes' impedance variation normalized to the last trial, their average over six subjects and also measured impedance in trial 8, normalized to the measured impedance at the last trial. We observe that Ag/AgCl electrodes are fairly stable and after releasing the pressure keep the impedance almost equal to the last time pressure is induced [average $(Z_8/Z_{11}) = 1.06$], whereas conductive textile shows the maximum variation in the first trial among all three electrode types. All electrodes are subject to irreversible changes and Z_8/Z_{11} ratio is close to one. Having the minimum value of this ratio compared to the other electrode types, conductive textile is the one which keeps the changes less than others.

TABLE III

MEASURED IMPEDANCE AT THE FIRST TRIAL (Z_1) AND THE LAST TIME PRESSURE IS APPLIED (Z_8) NORMALIZED TO THE LAST MEASUREMENT (Z_{11})

	Z_1/Z_{11} Range (f=30Hz)	Z_1/Z_{11} Average (f=30Hz)	Z_8/Z_{11} Range (f=30Hz)	Z_8/Z_{11} Average (f=30Hz)
Ag/AgCl	1.24 to 1.90	1.49	1.06 to 1.10	1.06
Conductive Textile	1.67 to 7	4.47	0.67 to 0.93	0.79
Orbital electrodes	0.92 to 7.06	2.74	0.95 to 1.01	0.98

To visualize how the circuit model components change during applying pressure and releasing it, they are plotted as a function of trial. These values are normalized to the values from the last trial.

TABLE IV

ESTIMATED ELECTRICAL COMPONENTS IN THE FIRST TRIAL ($P = 0$) AND THE LAST TIME PRESSURE IS APPLIED (TRIAL 8, $P = 4$ kPa) NORMALIZED TO THE LAST TRIAL (TRIAL11, $P = 0$)

	C_1/C_{11}	C_1/C_{11} Avg	C_8/C_{11} Avg	$(R_0)_1/(R_0)_{11}$	$(R_0)_1/(R_0)_{11}$ Avg	$(R_0)_8/(R_0)_{11}$ Avg	$R_{\infty 1}/R_{\infty 11}$	$R_{\infty 1}/R_{\infty 11}$ Avg	$R_{\infty 8}/R_{\infty 11}$ Avg
Ag/AgCl	0.96 to 1.15	1.05	1.02	1.28 to 2.99	1.75	1.08	0.98 to 1.08	1.03	1.01
Conductive Textile	0.14 to 1.00	0.46	1.50	2.03 to 6.75	3.74	0.75	0.12 to 1.66	1.02	0.94
Orbital electrode	0.05 to 0.70	0.40	0.97	0.64 to 4.42	2.03	1.00	1.06 to 2.08	1.27	1.01

Fig. 14 shows the variation of C per trial for six subjects and for all electrodes. For Ag/AgCl electrodes, C slightly increases and does not come back to its initial value after removing the pressure, as opposed to conductive textile and orbital electrodes which in them, C goes up when applying pressure and goes down when releasing it; however, it still remains higher than its previous value. This leads to a generally increasing irreversible trend for C in these two-electrode types. As Fig. 14 shows, we observe the strongest fluctuations of C in conductive textile. Ratio of C in the first trial to C in the last trial in Ag/AgCl electrodes varies from 0.96 to 1.15 from subject to subject and the average is equal to 1.05 while this ratio for conductive textile varies from 0.14 to 1.00 and the mean value is 0.46. For orbital electrodes this ratio varies from 0.05 to 0.70 with the average of 0.40 (Table IV).

Fig. 15 depicts the variation of R_0 per trial for six subjects and for all electrodes. As it can be observed in these graphs, R_0 keeps decreasing in Ag/AgCl electrodes, regardless of applying pressure or releasing it. In conductive textile electrodes, this component goes down with applying pressure and again goes up when releasing it, but it still remains lower than its previous value under pressure [Fig. 15(b)]. Therefore, it has a general decreasing trend. In orbital electrodes, R_0 keeps decreasing in applying pressure measurements and stays the same in the next nonpressure trial [Fig. 15(c)]. It also has a general decreasing trend in the entire process including eleven trials. In one subject (S_3), we observe an increasing trend for this component. Ratio of R_0 in the first trial to R_0 in the last trial in Ag/AgCl electrodes varies from 1.28 to 2.99 with the average of 1.75 and this ratio for conductive textile fluctuates from 2.03 to 6.75 and the average is equal to 3.74, while this ratio for orbital electrodes is in the range of 0.64 to 4.42 with the average of 2.03 (Table IV).

As electrical equivalent circuit (Fig. 3) shows, the skin-electrode impedance is dominated by R_0 at low frequencies. Noninvasive biosignals are comprised of primarily low frequencies (e.g., ECG $<$ 250 Hz, EMG $<$ 500 Hz, and EEG $<$ 150 Hz). Hence; R_0 is the parameter that determines the electrodes' behavior throughout these experiments. This parameter R_0 appears to have more sensitivity with dry electrodes (conductive textile and orbital) as compared to wet electrodes (Ag/AgCl); however, for many applications such as wearable devices, reusable dry electrodes are preferable [7], [53]. It does appear that the skin-electrode impedance remains relatively stable once an initial pressure is applied, even when it is removed after a while. This suggests that dry electrodes may have a lot of noise initially in a wearable devices but this noise level quickly reduces as the skin-electrode impedance stabilizes.

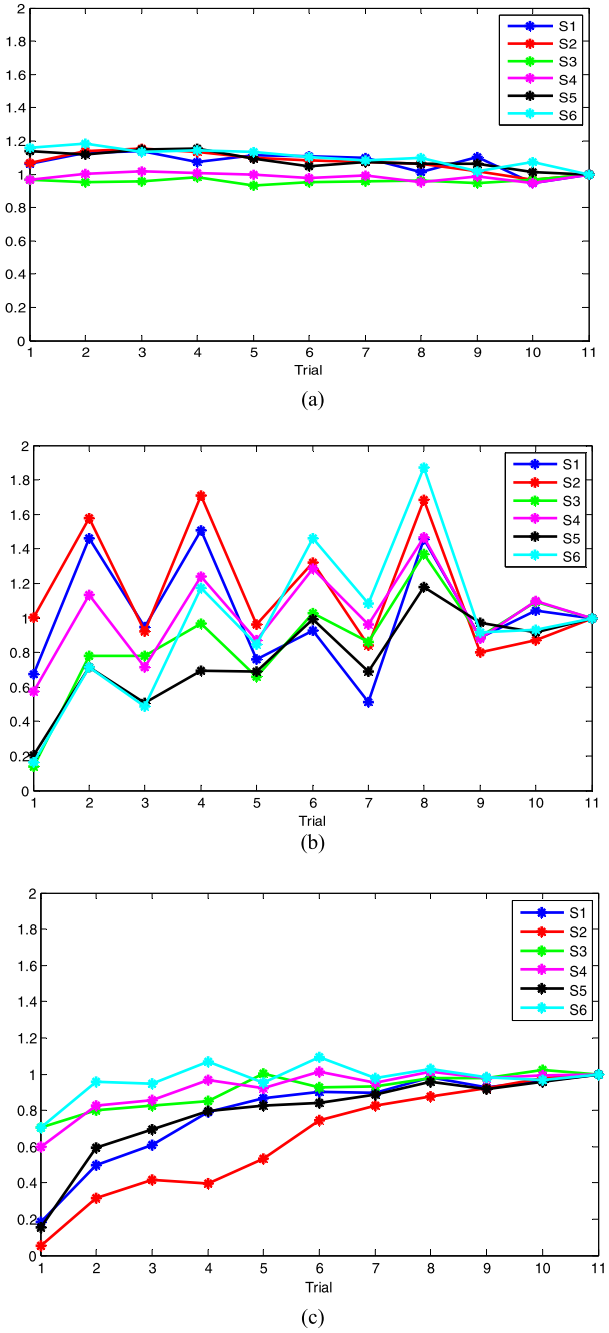

Fig. 14. (a) C Ag/C Ag (trial11), (b) C textile/C textile (trial11), and (c) C orbital/C orbital (trial11).

Fig. 16 depicts the variation of R_∞ per trial for six subjects and for all electrodes. R_∞ in Ag/AgCl and orbital electrodes do not show much change in pressure and nonpressure trials [Fig. 16(a) and (c)]. In conductive textile, R_∞ is affected by pressure with a modulation pattern consistent with the loading and unloading [Fig. 16(b)]. Ratio of R_∞ in the first trial to R_∞ in the last trial in Ag/AgCl electrodes varies from 0.98 to 1.08 with the average of 1.03 and this ratio for conductive textile varies from 0.12 to 1.66 and its average value for all six subjects is 1.02. This ratio for orbital electrodes varies

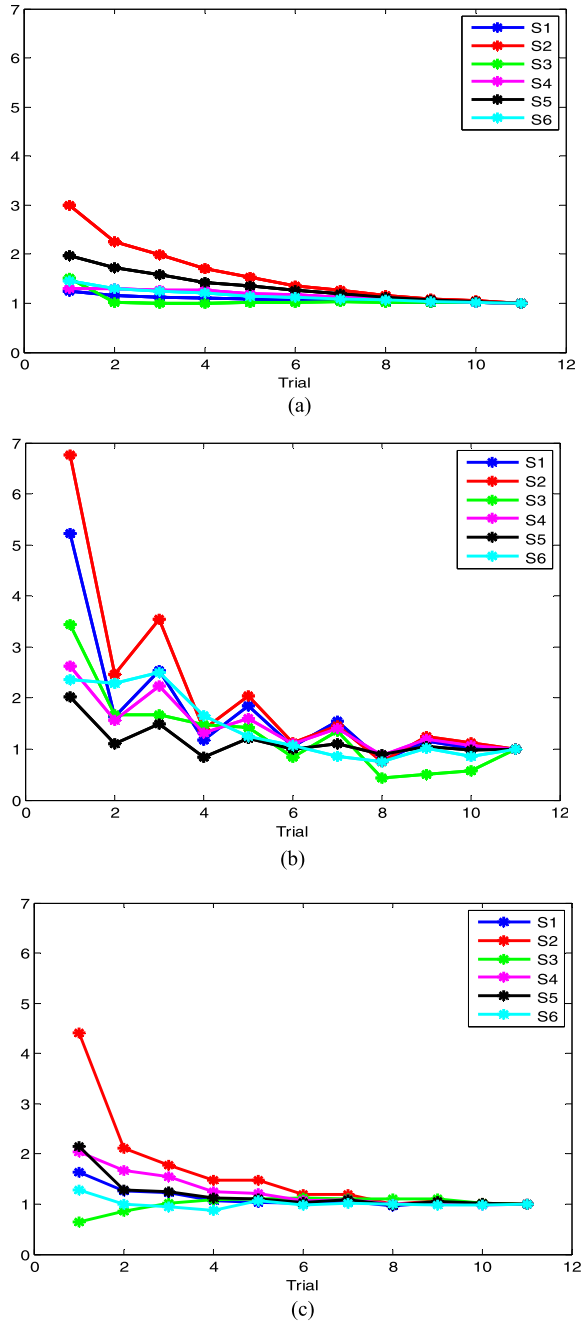

Fig. 15. (a) (R_0)Ag/ (R_0)Ag(trial11), (b) (R_0)textile/(R_0)TEXTILE(trial11), (c) (R_0)orbital/ (R_0)orbital(trial11).

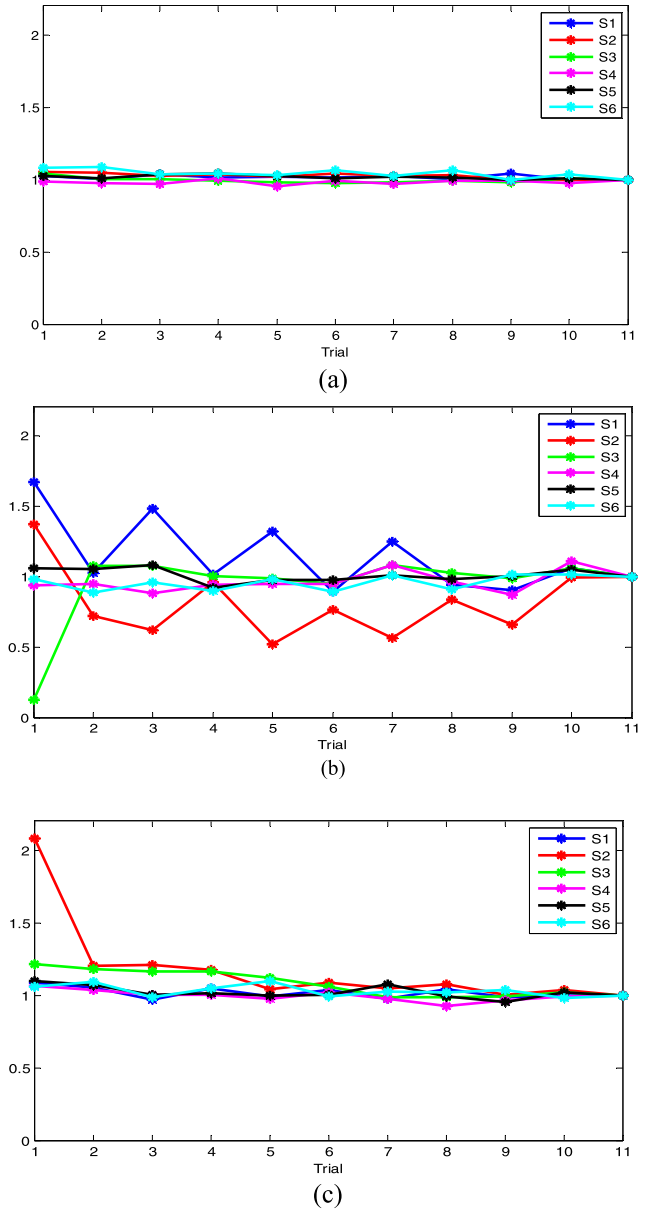

Fig. 16. (a) R_∞Ag/R_∞Ag(trial11), (b) R_∞textile/R_∞textile(trial11), and (c) R_∞orbital/R_∞orbital(trial11).

from 1.06 to 2.08 with the average equal to 1.01 (Table IV). Estimated components in the first trial ($P = 0$) and the last time pressure is applied (trial 8, $P = 4$ kPa) normalized to the last trial (trial11, $P = 0$) are also calculated and shown in Table IV.

Fig. 17 shows the variation of α in each trail for all subjects and three types of electrodes. In Ag/AgCl and orbital electrodes, α does not show much change in pressure and nonpressure trials and is almost stable. However, in textile electrodes changes are more readily observed. For four subjects out of six, α decreases under pressure and increases when unloading the pressure. Ratio of α in the first trial to α in the last trial in Ag/AgCl electrodes varies from 1.02 to 1.04 with the average of 1.02 and this ratio for conductive textile varies from 0.91 to 1.14 and its average value for all six subjects is 1.05. This ratio for orbital electrodes varies from 0.97 to 1.00 with the average equal to 0.99 (Table V).

Table IV is created to compare circuit model components changes due to the first pressure application and also their irreversible changes. Based on the results, R_∞ has the least variation among all components and R_0 appears to have the maximum variation. In addition, components corresponding to Ag/AgCl electrodes are the most stable ones and those of conductive textile have the maximum variation that is consistent with the previously presented results in Table III.

Results show that the application of an externally applied pressure tends to cause an increase in C values and a decrease in R_0 values. A plausible explanation for these trends is that

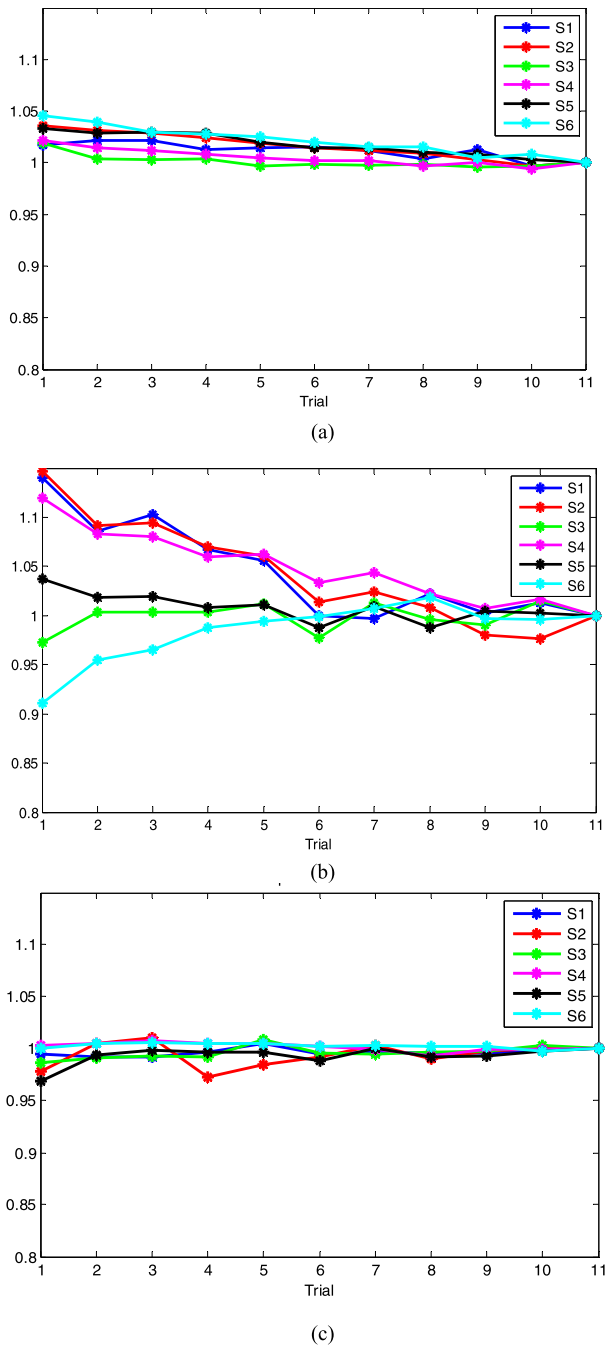

Fig. 17. (a)αAg/ αAg(trial11), (b) αtextile/αtextile(trial11), and (c) αorbital/αorbital(trial11).

the applied pressure results in a better contact between the electrode and the skin; therefore, the effective contact area is increased. The value of any capacitor can be expressed by the following formula:

$$C = \varepsilon_0 \varepsilon_r \frac{A}{d} \tag{2}$$

where C indicates the capacitance in Farad (F), ε_r is the dielectric constant of the material filling the distance between two parallel plates, ε_0 shows the electric constant (approximately 8.85×10^{-12} Fm^{-1}), A is the effective common area between two parallel plates (m^2), and d(m) is the distance between two parallel plates. Capacitance is directly proportional to the area

TABLE V

ESTIMATED α IN THE FIRST TRIAL ($P = 0$) AND THE LAST TIME PRESSURE IS APPLIED (TRIAL 8, $P = 4$ kPa) NORMALIZED TO THE LAST TRIAL (TRIAL11, $P = 0$)

	α_1/α_{11} Range	α_1/α_{11} Average	α_8/α_{11} Average
Ag/AgCl	1.02 to 1.04	1.02	1.00
Conductive Textile	0.91 to 1.14	1.05	1.01
Orbital electrodes	0.97 to 1.00	0.99	0.99

so if increased pressure results in effective surface contact area the capacitance will increase. It may also be the case that the pressure also decreases the distance between the two charged layers resulting in an increased capacitance.

Resistance of any material can be formulated as in

$$R = \rho \frac{l}{A} \tag{3}$$

where R is the resistance in ohm (Ω); ρ stands for the resistivity of the material with the dimension of ($\Omega \cdot$ m); L represents the length of the material with the dimension of (m); and A shows the cross-sectional area of the conductor material with the dimension of (m^2). Based on (3), resistance is inversely proportional to area, and if applying pressure makes the contact area larger it could explain why $R_0 - R_\infty$ tends to decrease with increased pressure. Another reason for this observation is that applying pressure was associated with increase sweat activity [43]. This increased sweat would result in a decrease in resistance.

R_∞ does not show significant or consistent changes for the Ag/AgCl and orbital electrodes. For the conductive textile it goes down when pressure is applied and goes up when pressure removed. As we mentioned in Section III-C, R_{tissue} is also incorporated in the estimation of R_∞, therefore its probable fluctuations due to the pressure could have masked any trend associated with R_∞. R_∞ is not important at low frequencies because it is relatively small ($R_\infty \ll R_0 - R_\infty$). It becomes a dominant term at high frequencies but this is well beyond the bandwidth of biosignals. Any changes observed are probably not important in terms of biosignal quality.

Variations of α are also consistent with our findings about other components, as it has a very small range of changes in Ag/AgCl and orbital electrodes, whereas it shows more deviations in textile electrodes. In general, α is very stable as shown in Table V.

For all electrodes, the skin-electrode impedance was lower for trial 11 ($P = 0$ kPa) than trial 1 ($P = 0$ kPa). Thus, the applied pressure resulted in an irreversible change in the skin-electrode impedance. This hysteresis effect is consistent with previous observations [44], [47]. A portion of the irreversible decrease in impedance can be attributed to electrode settling [6], [46], [47]; however, decreases in impedance are larger than what would be anticipated with electrode settling [44].

Ag/AgCl electrodes were observed have the lowest skin-electrode impedance and exhibited the least amount of effects to applied pressure. This result is likely due to the presence of the electrolytic gel, which is compliant and provides a good skin-electrode contact that is consistent across the applied pressures. Despite good performance, Ag/AgCl electrodes

might not be appropriate for wearable home health care devices. With long-term use, the gel may dry out and cause a large impedance to exist between the skin and electrode. From a usability perspective, a reusable system that does not require the need to apply gel to the electrodes may also be preferable. On the other hand, dry electrodes such as conductive textile and orbital electrodes are perhaps not appropriate for short-term applications, because they need time and some pressure to establish a stable connection. The effects of applied pressure are relatively large initially but diminish with subsequent applications of pressure, with the orbital electrodes performing better than the conductive textile.

V. Conclusion

How applied pressure influences the skin-electrode impedance was investigated for three types of electrodes in this paper. Employing skin-electrode circuit model, components corresponding to each trial were extracted and their variations through all of them were discussed. Large changes were observed in magnitude of the skin-electrode impedance, associated with the initial application of pressure. These changes were observed to be irreversible and sustaining themselves even after we released the pressure. Besides, we observed a general increasing trend for C and a decreasing trend for R_0. An increase in effective contact area is a reasonable hypothesis of why we observe such variations in C and R_0. These changes also appeared to be irreversible.

Ag/AgCl electrodes showed less variation throughout the entire process of applying and releasing pressure compared to dry electrodes (conductive textile and orbital electrodes). Therefore, from a practical point of view, Ag/AgCl electrodes seem relatively immune to changes in pressure. Dry electrodes skin-electrode impedance is modulated by pressure but there are irreversible changes, so the magnitude of the modulation decreases with successive applications and removal of pressure. As a result, biosignal recordings by dry electrodes may be initially poor, but will improve with time. This creates a problem with short recordings, unless skin preparation is performed, and less of a problem with long-term continuous monitoring applications such as wearable devices, where dry electrodes are preferred.

Findings in this paper are applicable and useful for researches targeting to minimize or eliminate the effects of the skin-electrode impedance in recorded signals, which can improve the quality of recorded signals, in turn making them more reliable especially for diagnostic purposes [11].

Future work will explore other potential influencing factors on the skin-electrode impedance, including sweat during exercise, and body weight. Besides; in the future, we will explore the physics behind the contact impedance such as how contact impedance forms and how skin structures interact with electrode. Moreover; the effects of pressure on this interaction in its physical sense will be studied in the future.

References

[1] *Pulse of the Industry—Medical Technology Report 2012 Power to the Patients: Point of View*. [Online]. Available: http://www.ey.com/GL/en/Industries/Life-Sciences/Pulse_medical-technology-report-2012

[2] Y.-L. Zheng *et al.*, "Unobtrusive sensing and wearable devices for health informatics," *IEEE Trans. Biomed. Eng.*, vol. 61, no. 5, pp. 1538–1554, May 2014.

[3] S. Patel, H. Park, P. Bonato, L. Chan, and M. Rodgers, "A review of wearable sensors and systems with application in rehabilitation," *J. Neuroeng. Rehabil.*, vol. 9, no. 21, pp. 1–17, 2012.

[4] C. De Capua, A. Meduri, and R. Morello, "A smart ECG measurement system based on Web-service-oriented architecture for telemedicine applications," *IEEE Trans. Instrum. Meas.*, vol. 59, no. 10, pp. 2530–2538, Oct. 2010.

[5] L. Fanucci *et al.*, "Sensing devices and sensor signal processing for remote monitoring of vital signs in CHF patients," *IEEE Trans. Instrum. Meas.*, vol. 62, no. 3, pp. 553–569, Mar. 2013.

[6] A. Searle and L. Kirkup, "A direct comparison of wet, dry and insulating bioelectric recording electrodes," *Physiol. Meas.*, vol. 21, no. 2, pp. 271–283, 2000.

[7] P. Laferriere, E. D. Lemaire, and A. D. C. Chan, "Surface electromyographic signals using dry electrodes," *IEEE Trans. Instrum. Meas.*, vol. 60, no. 10, pp. 3259–3268, Oct. 2011.

[8] Y. M. Chi, T.-P. Jung, and G. Cauwenberghs, "Dry-contact and noncontact biopotential electrodes: Methodological review," *IEEE Rev. Biomed. Eng.*, vol. 3, pp. 106–119, 2010.

[9] J. G. Webster, "Reducing motion artifacts and interference in biopotential recording," *IEEE Trans. Biomed. Eng.*, vol. BME-31, no. 12, pp. 823–826, Dec. 1984.

[10] H. de Talhouet and J. G. Webster, "The origin of skin-stretch-caused motion artifacts under electrodes," *Physiol. Meas.*, vol. 17, no. 2, pp. 81–93, 1996.

[11] B. Taji, S. Shirmohammadi, V. Groza, and I. Batkin, "Impact of skin–electrode interface on electrocardiogram measurements using conductive textile electrodes," *IEEE Trans. Instrum. Meas.*, vol. 63, no. 6, pp. 1412–1422, Jun. 2013.

[12] E. Richard and A. D. C. Chan, "Non-obtrusive electrocardiogram system for the smart rollator," in *Proc. IEEE Int. Symp. MeMeA*, Budapest, Hungary, May 2012, pp. 1–5.

[13] P. H. Devlin, R. G. Mark, and J. W. Ketchum, "Detection electrode motion noise in ecg signals by monitoring electrode impedance," *Comput. Cardiol.*, vol. 11, pp. 227–230, 1984

[14] P. S. Hamilton, M. G. Curley, R. M. Aimi, and C. Sae-Hau, "Comparison of methods for adaptive removal of motion artifact," in *Proc. Comput. Cardiol.*, Sep. 2000, pp. 383–386.

[15] B. Taji, S. Shirmohammadi, and V. Groza, "Measuring skin-electrode impedance variation of conductive textile electrodes under pressure," in *Proc. IEEE Int. Instrum. Meas. Technol.*, Montevideo, Uruguay, May 2014, pp. 1083–1088.

[16] K. S. Cole and R. H. Cole, "Dispersion and absorption in dielectrics I. Alternating current characteristics," *J. Chem. Phys.*, vol. 9, no. 4, pp. 341–351, 1941.

[17] S. Grimnes and O. G. Martinsen, "Cole electrical impedance model—A critique and an alternative," *IEEE Trans. Biomed. Eng.*, vol. 52, no. 1, pp. 132–135, Jan. 2005.

[18] D. H. Gordon, "Triboelectric interference in the ECG," *IEEE Trans. Biomed. Eng.*, vol. BME-22, no. 3, pp. 252–255, May 1975.

[19] J. Webster, *Medical Instrumentation: Application and Design*, 4th ed. Hoboken, NJ, USA: Wiley, 2009.

[20] S. Grimnes and O. Martinsen, *Bioimpedance and Bioelectricity Basics*, 2nd ed. Amsterdam, The Netherlands: Academic, 2008.

[21] E. Warburg, "About the behaviour of so-called 'impolarizable electrodes' the present alternating current," *Ann. Phys. Chem.*, vol. 67, pp. 493–499, 1899.

[22] L. A. Geddes, "Historical evolution of circuit models for the electrode-electrolyte interface," *Ann. Biomed. Eng.*, vol. 1, no. 25, pp. 1–14, 1997.

[23] C. Assambo, A. Baba, R. Dozio, and M. J. Burke, "Determination of the parameters of the skin-electrode impedance model for ECG measurement," in *Proc. 6th WSEAS Int. Conf. Electron., Hardw., Wireless Opt. Commun.*, 2007, pp. 90–95.

[24] D. Swanson and J. Webster, *A Model for Skin-Electrode Impedance*. San Diego, CA, USA: Academic, 1974, pp. 117–128.

[25] L. A. Geddes and M. E. Valentinuzzi, "Temporal changes in electrode impedance while recording the electrocardiogram with 'Dry' electrodes," *Ann. Biomed. Eng.*, vol. 1, no. 3, pp. 356–367, 1973.

[26] K. A. Kaczmarek and J. G. Webster, "Voltage-current characteristics of the electrotactile skin-electrode interface," in *Proc. Annu. Int. Conf. IEEE Eng. Med. Biol. Soc.*, Nov. 1989, pp. 1526–1527.

[27] B. R. Eggins, "Skin contact electrodes for medical applications," *Analyst*, vol. 118, no. 4, pp. 439–442, 1993.

[28] A. S. Elwakil and B. Maundy, "Extracting the Cole–Cole impedance model parameters without direct impedance measurement," *Electron. Lett.*, vol. 46, no. 20, pp. 1367–1368, Sep. 2010.
[29] J. Macdonald and E. Barsoukov, *Impedance Spectroscopy: Theory, Experiment, and Applications*. Hoboken, NJ, USA: Wiley, 2005.
[30] M. S. Spach, R. C. Barr, J. W. Havstad, and E. C. Long, "Skin-electrode impedance and its effect on recording cardiac potentials," *Circulation*, vol. 34, no. 4, pp. 649–656, 1966.
[31] G. Medrano, A. Ubl, N. Zimmermann, T. Gries, and S. Leonhardt, "Skin electrode impedance of textile electrodes for bioimpedance spectroscopy," in *Proc. 13th Int. Conf. Elect. Bioimpedance, 8th Conf. Elect. Impedance Tomogr.*, 2007, pp. 260–263.
[32] S. Grimnes, "Impedance measurement of individual skin surface electrodes," *Med. Biol. Eng. Comput.*, vol. 21, no. 6, pp. 750–755, 1983.
[33] L. A. Geddes and L. E. Baker, "The relationship between input impedance and electrode area in recording the ECG," *Med. Biol. Eng*, vol. 4, no. 5, pp. 439–449, 1966.
[34] D. P. Burbank and J. G. Webster, "Reducing skin potential motion artefact by skin abrasion," *Med. Biol. Eng. Comput.*, vol. 16, no. 1, pp. 31–38, 1978.
[35] H. W. Tam and J. G. Webster, "Minimizing electrode motion artifact by skin abrasion," *IEEE Trans. Biomed. Eng.*, vol. BME-24, no. 2, pp. 134–139, Mar. 1977.
[36] T. Yamamoto and Y. Yamamoto, "Electrical properties of the epidermal stratum corneum," *Med. Biol. Eng.*, vol. 14, no. 2, pp. 151–158, 1976.
[37] E. T. McAdams, J. Jossinet, A. Lackermeier, and F. Risacher, "Factors affecting electrode-gel-skin interface impedance in electrical impedance tomography," *Med. Biol. Eng. Comput.*, vol. 34, no. 6, pp. 397–408, 1996.
[38] K.-W. Kim, H.-Y. Choi, M.-H. Sim, I.-C. Jeong, and H.-R. Yoon, "Compensation on Impedance of the Stratum Corneum," *J. Elect. Eng. Technol.*, vol. 3, no. 3, pp. 444–449, 2008.
[39] R. Edelberg, "Relation of electrical properties of skin to structure and physiologic state," *J. Invest. Dermatol.*, vol. 69, no. 3, pp. 324–327, 1977.
[40] L. M. A. Nolan, J. Corish, and O. I. Corrigan, "Electrical properties of human stratum corneum and transdermal drug transport," *J. Chem. Soc., Faraday Trans.*, vol. 89, no. 15, pp. 2839–2845, 1993.
[41] I. Nicander and S. Ollmar, "Electrical impedance measurements at different skin sites related to seasonal variations," *Skin Res. Technol.*, vol. 6, no. 2, pp. 81–86, 2000.
[42] R. V. Hill, J. C. Jansen, and J. L. Fling, "Electrical impedance plethysmography: A critical analysis," *J. Appl. Physiol.*, vol. 22, no. 1, pp. 161–168, 1967.
[43] A. Karilainen, S. Hansen, and J. Müller, "Dry and capacitive electrodes for long-term ECG-monitoring," in *Proc. 8th Annu. Workshop Semiconductor Adv.*, vol. 17. Nov. 2005.
[44] A. Albulbul and A. D. C. Chan, "Electrode-skin impedance changes due to an externally applied force," in *Proc. IEEE Int. Symp. Med. Meas. Appl. (MeMeA)*, Budapest, Hungary, May 2012, pp. 1–4.
[45] R. Dozio, A. Baba, C. Assambo, and M. J. Burke, "Time based measurement of the impedance of the skin-electrode interface for dry electrode ECG recording," in *Proc. 29th Annu. Int. Conf. IEEE Eng. Med. Biol. Soc.*, Aug. 2007, pp. 5001–5004.
[46] A. Baba and M. J. Burke, "Measurement of the electrical properties of ungelled ECG electrodes," *Int. J. Biol. Biomed. Eng.*, vol. 2, no. 3, pp. 89–97, 2008.
[47] D. K. Swanson, "Pressure-induced changes in skin-through-electrode impedance," M.S. thesis, Dept. Electr. Eng., Univ. Wisconsin, Madison, WI, USA, 1972.
[48] K. E. Sparks and A. T. Rood, "A comparison of ECG signal quality between a novel dry electrode and standard gel electrode," *Med. Sci. Sports Exercise*, vol. 38, no. 1, p. S5, 2006.
[49] K.-P. Hoffmann and R. Ruff, "Flexible dry surface-electrodes for ECG long-term monitoring," in *Proc. 29th Annu. Int. Conf. IEEE Eng. Med. Biol. Soc.*, Aug. 2007, pp. 5739–5742.
[50] T. A. Kosierkiewicz, "Dry and flexible elastomer electrodes outperform similar hydrogel and Ag/AgCl electrodes," in *Proc. IEEE Int. Symp. Med. Meas. Appl. (MeMeA)*, May 2013, pp. 306–308.
[51] J. Muhlsteff *et al.*, "Wearable approach for continuous ECG—and activity patient-monitoring," in *Proc. 26th Annu. Int. Conf. IEEE Eng. Med. Biol. Soc.*, Sep. 2004, pp. 2184–2187.
[52] *Comparison of ECG Signal Quality Between a Novel Dry Electrode and a Standard Gel Electrode*. [Online]. Available: http://www.orbitalresearch.com/PDFs/ORI_ACSM_Abstract.pdf
[53] J. Muhlsteff and O. Such, "Dry electrodes for monitoring of vital signs in functional textiles," in *Proc. 26th Annu. Int. Conf. IEEE Eng. Med. Biol. Soc.*, Sep. 2004, pp. 2212–2215.

Bahareh Taji received the B.Sc. degree in electrical engineering from the Isfahan University of Technology, Isfahan, Iran, and the M.A.Sc. degree in biomedical engineering from the University of Ottawa, Ottawa, ON, Canada, in 2013, where she is currently pursuing the Ph.D. degree in biomedical engineering.

Her current research interests include biomedical signal processing and quality assessments, machine learning and pattern classification.

Adrian D. C. Chan (S'93–M'03–SM'06) received the B.A.Sc. degree in computer engineering from the University of Waterloo, Waterloo, ON, Canada, in 1997, the M.A.Sc. degree in electrical engineering from the University of Toronto, Toronto, ON, Canada, in 1999, and the Ph.D. degree in electrical engineering from the University of New Brunswick, Fredericton, NB, Canada, in 2003.

He has served as the Associate Dean of Programs and Awards at the Faculty of Graduate and Post-Doctoral Affairs, Carleton University, Ottawa, ON, Canada, the Director of the Ottawa-Carleton Institute for Biomedical Engineering, Ottawa, ON, Canada, the Vice President of the Canadian Medical and Biological Engineering Society, Ottawa, ON, Canada, and a Co-Founder of NeuroQore Inc., Ottawa, ON, Canada. He is a Registered Professional Engineer with Professional Engineers Ontario, Toronto, ON, Canada. He is currently a Professor with the Department of Systems and Computer Engineering, the Assistant Vice President (Academic) with Carleton University, and the Director of the NSERC CREATE Research and Education in Accessibility, Design, and Innovation Training Program, Ottawa, ON, Canada. His current research interests include biological signal processing, signal quality assessments, biomedical image processing, pattern recognition, assistive devices, and noninvasive sensor systems.

Dr. Chan is a member of the IEEE Engineering in Medicine and Biology Society, the Canadian Medical and Biological Engineering Society, and the Biomedical Engineering Society. He is a 3M Teaching Fellow.

Shervin Shirmohammadi (M'04–SM'04–F'17) received the Ph.D. degree in electrical engineering from the University of Ottawa, Ottawa, ON, Canada.

He is currently a Professor with the School of Electrical Engineering and Computer Science, University of Ottawa, where he is also the Director of the Distributed and Collaborative Virtual Environment Research Laboratory, involved in the research in multimedia systems and networks, including measurement techniques for network, video streaming, and health systems. The results of his research, funded by more than $13 million from public and private sectors, have led to over 300 publications, including over 70 journal papers, over 65 researchers trained at the Post-Doctoral, Ph.D., and master's levels, holds 20 patents and technology transfers to the private sector, and a number of awards.

Dr. Shirmohammadi was a member of the IEEE I^2MTC Board of Directors from 2014 to 2016. He has been an IMS AdCom Member since 2014. He is a Lifetime Senior Member of the ACM, a University of Ottawa Gold Medalist. He is currently the Editor-in-Chief of the IEEE TRANSACTIONS ON INSTRUMENTATION AND MEASUREMENT, and an Associate Editor of *ACM Transactions on Multimedia Computing, Communications, and Applications* and the IEEE TRANSACTIONS ON CIRCUITS AND SYSTEMS FOR VIDEO TECHNOLOGY. He was the Associate Editor-in-Chief of the IEEE TRANSACTIONS ON INSTRUMENTATION AND MEASUREMENT in 2013 and 2016, IEEE INSTRUMENTATION AND MEASUREMENT MAGAZINE in 2014 and 2015, and the *Journal of Multimedia Tools and Applications* (Springer) from 2004 to 2012.He has been served as the Vice President of its Membership Development Committee since 2014. He is currently a Licensed Professional Engineer in Ontario.